MOLECULAR AND CELLULAR BIOLOGY, Sept. 2001, p. 5970–5978 Vol. 21, No. 17
0270-7306/01/$04.00+0 DOI: 10.1128/MCB.21.17.5970–5978.2001

Neurocan Is Dispensable for Brain Development

XIAO-HONG ZHOU,[1] CORD BRAKEBUSCH,[1] HENRY MATTHIES,[2] TOSHITAKA OOHASHI,[3] EMILIO HIRSCH,[3] MARKUS MOSER,[4] MANFRED KRUG,[2] CONSTANZE I. SEIDENBECHER,[5] TOBIAS M. BOECKERS,[5,6] UWE RAUCH,[1] REINHARD BUETTNER,[4] ECKART D. GUNDELFINGER,[5] AND REINHARD FÄSSLER[1,3]*

Department of Experimental Pathology, Lund University, 221 85 Lund, Sweden,[1] and Institute for Pharmacology and Toxicology, Otto von Guericke University, 39120 Magdeburg,[2] Max Planck Institute for Biochemistry, 82152 Martinsried,[3] Institute of Pathology, University Hospital of RWTH Aachen, 52074 Aachen,[4] Leibniz Institute for Neurobiology, 39118 Magdeburg,[5] and AG Molecular Neurobiology, Institute for Anatomy, Westfälische Wilhelms-Universität, 48149 Münster,[6] Germany

Received 23 April 2001/Accepted 30 May 2001

Neurocan is a component of the extracellular matrix in brain. Due to its inhibition of neuronal adhesion and outgrowth in vitro and its expression pattern in vivo it was suggested to play an important role in axon guidance and neurite growth. To study the role of neurocan in brain development we generated neurocan-deficient mice by targeted disruption of the neurocan gene. These mice are viable and fertile and have no obvious deficits in reproduction and general performance. Brain anatomy, morphology, and ultrastructure are similar to those of wild-type mice. Perineuronal nets surrounding neurons appear largely normal. Mild deficits in synaptic plasticity may exist, as maintenance of late-phase hippocampal long-term potentiation is reduced. These data indicate that neurocan has either a redundant or a more subtle function in the development of the brain.

The extracellular matrix of the brain is suggested to play an important role during development of the nervous tissue, especially in axon guidance of neurons (44). The interstitial matrix of the brain has a unique composition compared to other tissues of the body. It consists mainly of hyaluronic acid, proteoglycans, and tenascins (32), while it lacks components present in the interstitial matrix of other tissues, such as fibrillar collagens and fibronectin. However, some extracellular matrix molecules which are missing in adult brain, such as fibronectin, are transiently expressed during development (35).

Neurocan is a proteoglycan prominently expressed in brain (41). Recent findings show that it is also expressed by cells of the hematopoietic system (33). During early postnatal development neurocan accounts for at least 20% of the protein of the soluble brain proteoglycans (41). The protein backbone with a molecular mass of about 130 kDa is decorated with 5 to 6 N-linked and up to 40 O-linked oligosaccharides and about three chondroitin sulfate chains. Neurocan belongs to the lectican family of proteoglycans, which contain an N-terminal hyaluronan binding domain, a C-terminal lectin-like domain, and a central glycosaminoglycan attachment region lacking any significant homology with other family members (17, 38). All members of this family—aggrecan, neurocan, versican, and brevican—are expressed in brain, but with different developmental expression profiles (26).

In rat brain neurocan protein is first detected at embryonic day 12 (E12). The expression of neurocan increases during late embryogenesis but decreases significantly within the first month after birth (22). During development an increasing fraction of neurocan undergoes proteolytic processing, resulting in core glycoproteins of 130 and 150 kDa (19). In addition, the size of the chondroitin side chains and their type of sulfation change postnatally (39). How this processing affects the biological function of neurocan is not known.

Neurocan has been shown to interact and colocalize with tenascin-C in cerebellum at postnatal day 7 (D7) (11, 38). Furthermore, it binds with high affinity to the neural cell adhesion molecules Ng-CAM/L1 (10), axonin (27), and N-CAM (42), which show an overlapping expression with neurocan. The N-terminal domain of neurocan mediates the binding to hyaluronan (43). As in the binding between aggrecan and hyaluronan (30), this interaction might be stabilized by link protein, which copurifies with neurocan from brain (23). In addition, evidence exists that the C-type lectin domain at the C terminus has affinity for sulfatides, sulfated cell surface glycolipids (28). These interactions should enable neurocan to participate in a network consisting of tenascin-C, hyaluronic acid, and cell surface components.

Neurocan was shown to inhibit Ng-CAM and N-cadherin-mediated neuronal adhesion and neuronal growth in vitro (8, 16). It also prevents glial adhesion to Ng-CAM but not to tenascin-C (17). Furthermore, some expression studies indicated an accumulation of neurocan in certain brain regions that are avoided by axons (14, 45). These data led to the suggestion that neurocan may act as a barrier to axonal growth, thus playing an important role in axon guidance and neurite growth during brain development.

To test this hypothesis we generated mice with a targeted inactivation of the neurocan gene and studied the effect of the lack of this molecule.

MATERIALS AND METHODS

Generation of neurocan-deficient mice. Targeting constructs to inactivate the mouse neurocan gene were made using a cosmid clone of the mouse neurocan gene described earlier (40). For the NC*Ig* construct, a 11.2-kb *Spe*I-*Xho*I fragment containing the promoter region and exons 1 to 3 was fused to a thymidine kinase expression cassette. To inactivate the neurocan gene, a neomycin resis-

* Corresponding author. Mailing address: Department of Experimental Pathology, Lund University, 221 85 Lund, Sweden. Phone: 46 46 173400. Fax: 46 46 158202. E-mail: Reinhard.Fassler@pat.lu.se.

tance expression cassette was inserted into a unique *Bst*EII site within exon 3, which encodes the immunoglobulin-like domain. For the NC*LacZ* construct, the 4.3-kb *Stu*I-*Bst*EII fragment of the 11.2-kb *Spe*I-*Xho*I fragment, containing part of exon 1, exon 2, and part of exon 3, was replaced by a promoterless NTR-*lacZ* gene followed by a neomycin expression cassette. For the NC*Cre* construct, the 7.6-kb *Kpn*I-*Sac*I fragment of the 11.2-kb *Spe*I-*Xho*I fragment, which contains the TATA box, transcription initiation site, exon 1, and exon 2, was replaced by a *loxP-neo-tk-loxP* cassette. The three constructs were linearized and electroporated into R1 embryonic stem cells as described earlier (7). After selection for stable transfectants with G418, homologous recombinants were identified by Southern blot analysis. Two of the positive clones of the NC*Cre* construct were transiently transfected with a *Cre* expression plasmid (a gift from Werner Müller, University of Cologne, Cologne, Germany) and selected with 2′-fluoro-2′-deoxy-1β-D-arabinofuranosyl-5-iodouracil. Two clones from each construct were then injected into C57BL/6 blastocysts, and injected blastocysts were transferred into pseudopregnant foster mothers. The resulting chimeric mice were tested for germ line transmission and used for establishment of 129Sv inbred lines and 129Sv/C57BL/6 outbred lines.

Immunohistochemistry, electron microscopy, and LacZ staining. Immunohistochemical staining of brain sections fixed with 4% paraformaldehyde (PFA) in phosphate-buffered saline (PBS) was done according to standard procedures. Rabbit antisera raised against rat brain-derived and recombinant (for booster injections) rat neurocan, against recombinant rat brevican, and against recombinant mouse tenascin-C (generous gifts from R. Timpl, Martinsried, Germany) were used. Staining of perineuronal nets with *Wisteria floribunda* lectin was performed exactly as described (3).

LacZ staining was carried out as described earlier (7). In brief, the 8-μm-thick sagittal brain cryosections were fixed in 0.2% glutaraldehyde in 0.1 M K_2HPO_4 (KPP) containing 5 EGTA and 2 $MgCl_2$, pH 7.4, for 5 min; washed in 0.1 M KPP containing 0.01% sodium deoxycholate and 0.02% NP-40 (three times, for each at room temperature); and for 5 min stained in 0.1 M KPP containing X-Gal (5-bromo-4-chloro-3-indolyl-β-D-galactopyranoside) (0.5 mg/ml), 10 mM $K_3[Fe(CN)_6]$, and 10 mM $K_4[Fe(CN)_6]$ at 37°C overnight protected from light.

For electron microscopy, mice were perfused with Karnovsky's solution (2.2% glutaraldehyde and 2.5% paraformaldehyde in 0.1 M phosphate buffer [pH 7.35]). Brains were dissected and cut on a Vibratome (200-μm-thick sections) in sagittal orientation. Subsequently the hippocampal CA1 region was carefully removed, postfixed in 1% OsO_4, dehydrated in alcohol, and embedded in Epon. Ultrathin sections were contrasted with uranyl acetate and lead citrate and examined with a Philips electron microscope.

In situ hybridization. Pregnant Naval Marine Research Institute mice were perfused with 4% PFA–0.5% glutaraldehyde in 0.15 M cacodylate buffer. Embryos were dissected and postfixed for 2 h in the same solution. In situ hybridization of paraffin-embedded sections was essentially performed as described by Moser et al. (31). Briefly, slides were pretreated with proteinase K (1 to 10 μg/ml) for 30 min at 37°C, postfixed for 5 min in 4% PFA in PBS, washed twice in diethyl pyrocarbonate-H_2O, and acetylated in acetic anhydride diluted 1:400 in 0.1 M triethanolamine (pH 8.0) for 10 min at room temperature. Finally, slides were washed twice with diethyl pyrocarbonate-H_2O, dehydrated in ethanol, air dried, and prehybridized for 4 h at 50°C in a solution containing 50% formamide, 10% dextran sulfate, 10 mM Tris (pH 8.0), 10 mM NaPi, 2× SSC (1× SSC is 0.15 M NaCl plus 0.015 M sodium citrate), 5 mM EDTA, tRNA (150 μg/ml), 10 mM dithiothreitol, and 10 mM β-mercaptoethanol. Hybridizations were performed in the same solution supplemented with 50,000 cpm of sense or antisense riboprobe per μl at 50°C overnight. The RNA probes were prepared by in vitro transcription of neurocan cDNA with T3 or T7 RNA polymerase and ^{35}S-dUTP. The slides were washed twice at 55°C with 50% formamide–2× SSC–20 mM β-mercaptoethanol for 30 min and again in 2× SSC for 5 min. After treatment with RNase A (20 μg/ml) for 30 min at 37°C, slides were washed again five times as described before, finally rinsed in 2× SSC, dehydrated, coated with Kodak NTB2 emulsion, and left in darkness for 2 weeks.

Northern blotting. Total RNA was isolated from tissues and brains of embryos at various days of gestation and also from adult brains as described by Auffray and Rougeon (2). Northern blotting was carried out according to standard protocols. For hybridization mouse neurocan cDNA (nucleotides 30 to 730), mouse brevican cDNA (nucleotides 2160 to 2450), a 1,340-bp *Apa*I/*Hin*dIII mouse tenascin-C cDNA fragment spanning the 3′ coding region, mouse glyceraldehyde-3-phosphate dehydrogenase (GAPDH) cDNA, and mouse β-actin cDNA were used.

Western blotting. For developmental expression analysis, the soluble proteoglycan fraction of the brain was isolated. Neurocan was detected by Western blotting with rabbit antiserum raised against a recombinant C-terminal fragment of rat neurocan (starting with threonine 950). Briefly, mouse brain was homogenized in 5 volumes of 20 mM Tris-HCl (pH 8.0)–150 mM NaCl–5 mM EDTA–5 mM benzamidine–5 mM *N*-ethylmaleinimide–1 mM phenylomethylsulfonyl fluoride. After 15 min of centrifugation at 10,000 × *g*, Triton X-100 was added to the supernatant to a final concentration of 0.5%. Proteoglycans were separated by batch anion exchange chromatography using 1/10 volume of DEAE-Sephacel matrix, which was consecutively washed with homogenization buffer containing 0.1% Triton X-100, and homogenization buffer containing 250 mM NaCl and 0.1% 3-[(3-cholamidopropyl)-dimethylammonio]-1-propanesulfonate (CHAPS). The DEAE-matrix was eluted two times with 1 volume of homogenization buffer containing 1 M NaCl–0.1% CHAPS. The pooled eluates were dialyzed against 20 mM Tris-HCl (pH 8.0)–6 mM sodium acetate, lyophilized, and reconstituted in one-fifth of the original volume. Samples for sodium dodecyl sulfate-polyacrylamide gel electrophoresis (SDS-PAGE) were digested with 20 to 50 mU of Chondroitinase ABC. SDS-PAGE and Western blotting on nitrocellulose membranes with alkaline phosphatase-conjugated secondary antibodies and nitroblue tetrazolium–5-bromo-4-chloro-3-indolylphosphate substrate were performed as described (39).

For the analysis of the knockout mice rabbit antisera raised against rat brain-derived and recombinant (for booster injections) rat neurocan, against recombinant rat brevican, and against recombinant mouse tenascin-C (generous gifts from R. Timpl) were used. Briefly, mouse brains were homogenized in the same buffer as mentioned above. For the proteoglycan analysis all soluble molecules (i.e., molecules not sedimented after 10 min at 15,000 × *g*) were adjusted to 30 mM NaAc–100 mM Tris-Cl (pH 8.0) and treated with 1 mU of protease-free Chondroitinase ABC (15 μl [~30 μg of protein]) for 45 min at 37°C. Samples were substituted with nonreducing SDS sample buffer and analyzed for their protein content. Thirty micrograms of protein was applied per lane for SDS-PAGE analysis. Total homogenates were sonified twice for 20 s each, substituted with nonreducing SDS sample buffer, and analyzed for protein content. Fifty micrograms of protein was applied per lane for SDS-PAGE analysis under reducing conditions. SDS-PAGE and Western blotting on polyvinylidene difluoride membranes with peroxidase-conjugated secondary antibodies and en-

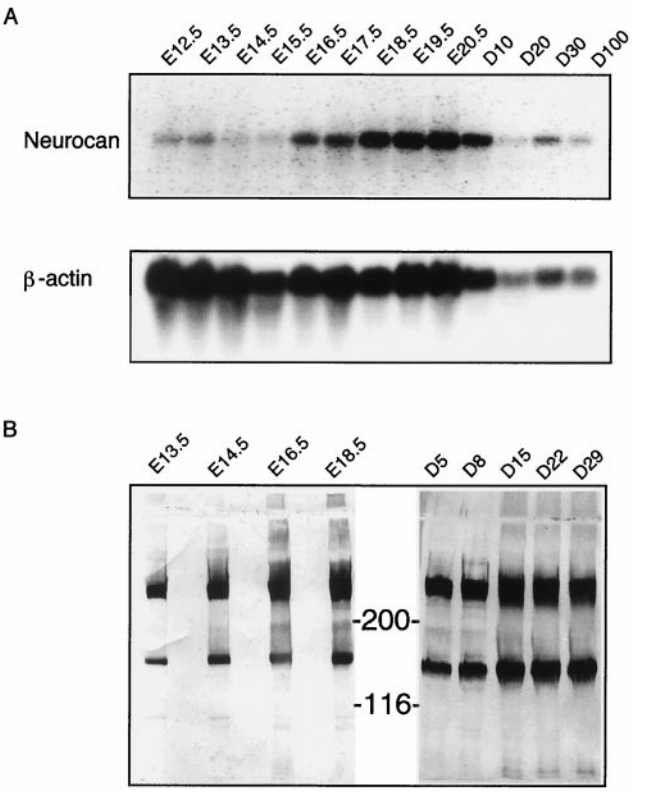

FIG. 1. The expression of neurocan gene and protein during mouse development. (A) Northern blot of the brain total RNA from E12.5 to D100 hybridized with a neurocan cDNA probe. β-Actin is the loading control. (B) Western blot of brain homogenates from E13.5 to D29 developed with antineurocan polyclonal antibody.

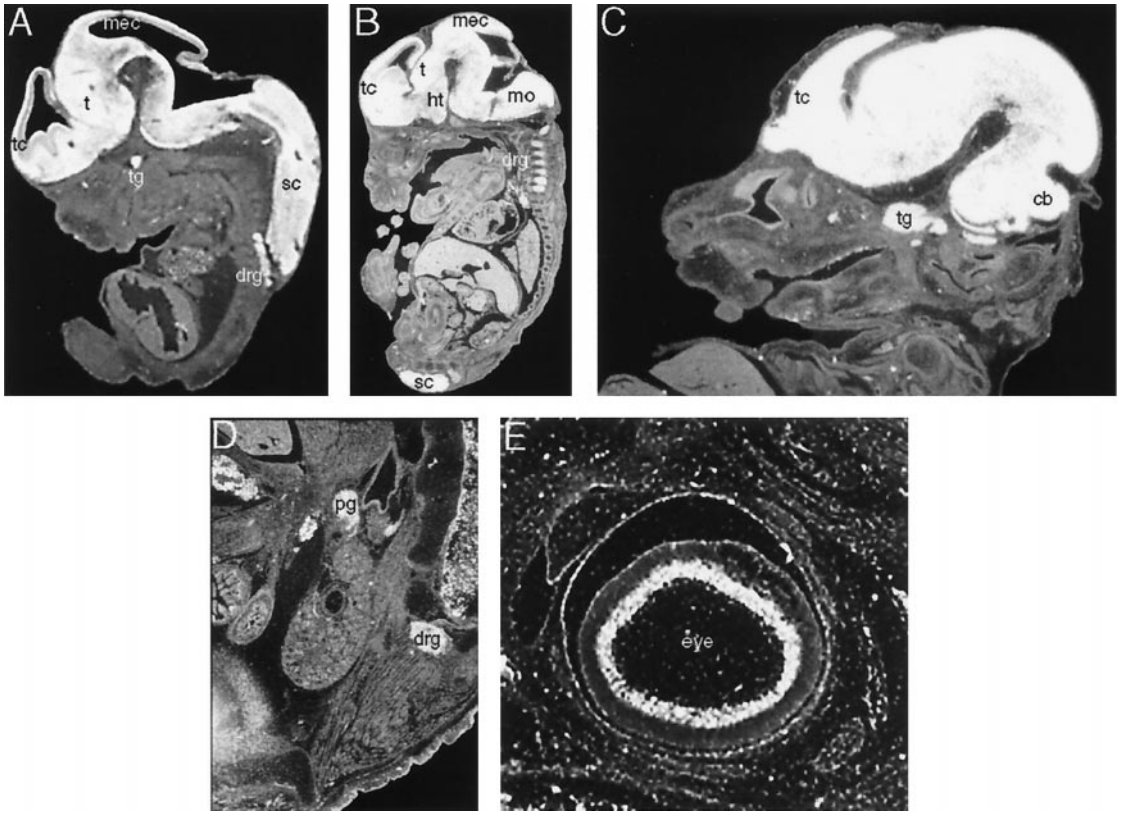

FIG. 2. In situ hybridization of neurocan transcript during embryonic stages. The positive signals are present in the telencephalon (tc), thalamus (t), hypothalamus (ht), mesencephalon (mec), medulla oblongata (mo), cerebellum (cb), trigeminal ganglion (tg), spinal cord (sc), and dorsal root ganglion (drg) at E12.5 (A), E13.5 (B), and E14.5 (C). At E16.5, the neurocan mRNA is also seen in the peripheral ganglion (pg) above the kidney (D) and expressed in the eye (E).

hanced chemiluminescence substrate were performed according to standard protocols.

Electrophysiology. Electrophysiological recordings in the CA1 region of the hippocampus of adult male mice were performed as described earlier (20). Briefly, 400-μm-thick transverse hippocampal slices were superfused with artificial cerebral spinal fluid (ACSF) saturated with 95% O_2–5% CO_2 and kept at 35°C. For separate recording of the field excitatory postsynaptic potential (EPSP) slope (fEPSP) and population spike amplitude (POP spike), glass recording electrodes were filled with ACSF and inserted into the basal dendritic and pyramidal layers of the CA1 region. Long-term potentiation (LTP) was induced by tetanization of the Schaffer collaterals with three 100-Hz-stimulus trains, each containing 50 pulses at double pulse width (0.2 ms half-width), with a 5-min interval between the trains. In order to follow the time course of LTP, test potentials were recorded every 5 to 10 min until 5 h after tetanization.

In a separate series of experiments, after 30 min of recording of the POP spike under control conditions, slices were perfused with a medium containing a 50 μM concentration of the GABA antagonist picrotoxin (PTX) for 30 min. Field potentials were further recorded until 4 h after the beginning of the PTX application.

Statistics. Statistics were carried out with the two-tailed Mann-Whitney U test. The results are shown as percent deviation of the actual records from baseline ± standard error of the mean.

RESULTS

Developmental expression of neurocan. To thoroughly assess the developmental expression of neurocan in mouse, Northern blotting, in situ hybridization and Western blotting were carried out. Neurocan mRNA could be detected in mouse brain first at E10 using Northern blotting (data not shown). After an intermediate downregulation at E14.5 to E15.5, it increased again, reaching its highest levels around birth (Fig. 1A). In adult mice, expression of neurocan mRNA was downregulated again. Enriched by ion-exchange chromatography and treated with chondroitinase, neurocan core proteins could be observed at all analyzed time points from E13 to D29 (Fig. 1B). The intensity of the staining indicated an increasing expression during embryonic development and a slowly progressing proteolytic processing of the neurocan protein postnatally. At all stages both major core protein bands, at about 150 and 250 kDa, were clearly present, and from E16 to D8 a faint third band at about 190 kDa could also be recognized.

In situ hybridization of embryos at different stages (Fig. 2) and Northern analysis of different tissues in adult mice (data not shown) revealed that the expression of neurocan was restricted to the central and peripheral nervous tissue. At E12.5 and E13.5, both dorsal root ganglia (Fig. 2A and B) and trigeminal ganglion (Fig. 2A to C) contained neurocan mRNA evenly distributed. In brain, neurocan expression was confined to the telencephalon (Fig. 2B and C), thalamus, spinal cord (Fig. 2A), the roof of the mesencephalon (Fig. 2B and C), the hypothalamus (Fig. 2B), and the cerebellum (Fig. 2C). At E16, neurocan transcripts were also observed in the peripheral ganglion above the kidney (Fig. 2D) and in the eye (Fig. 2E). Sense probes never showed signals in brain or spinal cord. These data show that neurocan expression is regulated during mouse development and that it is widespread, but not ubiquitous, in brain.

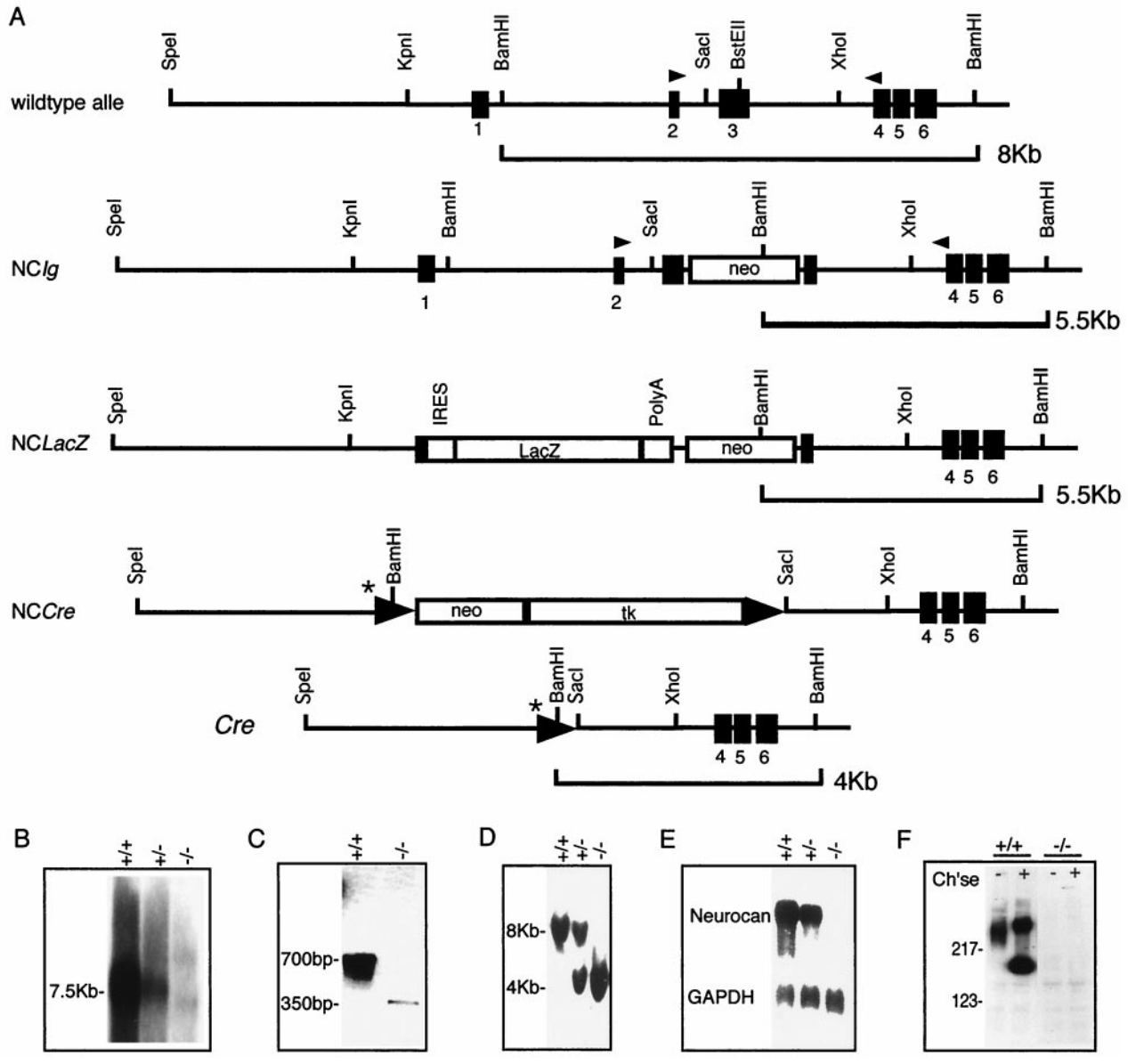

FIG. 3. Targeting strategy, Northern blot, RT-PCR, Southern blot, and Western blot. (A) Structure of the wild-type neurocan allele, targeting constructs, targeted neurocan allele after *cre-loxP*-mediated deletion, and the fragments digested with *Bam*HI. The black boxes show the exons of neurocan gene; the open boxes show the *neo, neo-tk*, and *lacZ* cassette; the small triangles show the primers for RT-PCR; and the *loxP* sites are indicated by large triangles. (B) Northern blot of total brain RNA of wild-type (+/+), heterozygous (+/−), and homozygous mutant mice (−/−) of the NC*Ig*-targeted mice. (C) RT-PCR of wild-type and homozygous mutant mice of the NC*Ig*-targeted strain amplified by the primers that are indicated in panel A. (D) Southern blot analysis of the *Bam*HI-digested genomic DNA derived from wild-type, heterozygous, and homozygous mice from the NC*Cre*-targeted strain. (E) Northern blot hybridization of neurocan gene derived from wild-type, heterozygous, and homozygous animals of NC*Cre* mutant strain. GAPDH is the loading control. (F) Western blot of brain homogenate extracted from 10-day-old wild-type and mutant mice of NC*Cre* treated with (+) and without (−) chondroitinase ABC (ch'se).

Generation of neurocan-deficient mice. By introducing a neomycin expression cassette into the exon 3 of the neurocan gene (construct NC*Ig*) (Fig. 3A), mutant mice were generated that showed no detectable protein levels of neurocan (data not shown), but a Northern blot of total brain RNA showed hybridization to a neurocan probe (Fig. 3B). Reverse transcription (RT)-PCR revealed that this neurocan transcript was made by alternative splicing of exon 2 to exon 4 (Fig. 3A) (NC*Ig*), omitting the immunoglobulin-like domain expressing exon 3 (Fig. 3C). To assure a complete ablation of neurocan expression, two additional null mice lines were established. The second knockout was construct NC*LacZ* (Fig. 3A), in which exon 2 and parts of exon 1 and 3 were replaced by a promoterless internal ribosome entry site-*lacZ* reporter gene. In mice carrying this mutation neither neurocan protein nor mRNA could be detected (data not shown). The second null mutation was made with construct NC*Cre* (Fig. 3A), in which the TATA box, transcription initiation site, exon 1, and exon 2 were replaced by a *neo-tk* cassette flanked with *loxP* sites (36). After recombinant embryonic stem cell clones were isolated

TABLE 1. Progeny of neurocan heterozygous crosses

Genotyping or targeting construct	No. (%) of progeny[a]			
	+/+	+/−	−/−	Total no. of progeny
NC*Ig*	58 (22)	146 (55)	60 (23)	264
NC*LacZ*	22 (29)	28 (37)	26 (34)	76
NC*Cre*	51 (24)	97 (45)	66 (31)	214

[a] +/+, wild type; +/−, heterozygous; −/−, homozygous.

the cassette was deleted by a transient *Cre* transfection. Neither the mRNA (Fig. 3E) nor the protein (Fig. 3F) of neurocan was detected in NC*Cre*-null mutant animals.

Both mutant strains were viable and fertile and showed no obvious behavioral abnormality (i.e., no abnormality of general activity, posture, social behavior, or holding reflexes). Heterozygous matings produced the expected numbers of homozygous, heterozygous, and wild-type mice 4 weeks after birth (Table 1), indicating no increased lethality of neurocan-null embryos.

No obvious defect in brain morphology of neurocan-null mice. To analyze brain morphology, Nissl staining of brain sections from 10- and 30-day-old mice was carried out. No difference was detected between neurocan-deficient mice and heterozygous or wild-type mice (data not shown).

Mice carrying the NC*LacZ* mutation were analyzed for β-galactosidase activity in brain sections. LacZ staining in the brain of null mutant mice was present in the hippocampus (Fig. 4B) and the cerebellum (data not shown) corresponding to the transcriptional activity of the neurocan gene.

Ultrastructural investigation of the hippocampal CA1 region revealed no obvious differences concerning size, density, and general appearance of synapses (Fig. 4K and L). After staining with *W. floribunda* lectin the perineuronal nets, a specialized form of extracellular matrix in the brain (4), were visualized in the cortex of wild-type and neurocan-null mice (Fig. 4I and J). The general appearance and frequency of these net-like structures were similar in mutant and wild-type brains.

No obvious compensatory upregulation of brevican and tenascin-C. Since the brain-specific proteoglycan brevican is closely related to neurocan (49), we tested whether the ablation of the neurocan gene results in a compensatory upregulation of brevican expression. Furthermore, we assessed whether the expression of the neurocan binding molecule tenascin-C (11, 38) is changed in the neurocan-null mice. Analyzing mRNA expression by Northern blotting showed no significant change in the mRNA levels of brevican and tenascin-C between wild-type, heterozygous, and homozygous mutant mice (Fig. 5A). Immunohistochemical stainings of tissue sections revealed that neurocan was present in the molecular layer of the hippocampus (Fig. 4C) in normal mice and absent in brain sections from mutant mice (Fig. 4D). Staining with the polyclonal antibodies against brevican core protein and tenascin-C showed that these molecules are located in the molecular layer of the hippocampus (Fig. 4E and G). The expression levels of both brevican and tenascin-C were similar in normal and neurocan-null brain sections (Fig. 4F and H). In addition, Western blot analysis of proteoglycans contained in the soluble protein fraction of brains of 10- and 30-day-old mice revealed no obvious counter-regulation of brevican either (Fig. 5B). For a quantitative assessment of tenascin-C content total brain homogenates of normal and neurocan-deficient mice were analyzed by immunoblotting. No obvious upregulation of tenascin-C (Fig. 5C) was apparent.

Plasticity of synapses in the CA1 region of the hippocampus. To study the synaptic performance in neurocan-deficient animals, synapses between Schaffer collaterals and principal pyramidal neurons of the CA1 region were characterized in hippocampal slice preparations using routine protocols (20). No significant differences were detectable in basic synaptic transmission, e.g., input-output curve and paired-pulse facilitation (data not shown). In contrast, maintenance of LTP was disturbed to some extent. While tetanic stimulation of CA1 pyramidal cells induced a rapid and profound synaptic potentiation in slices from homozygous neurocan-deficient mice, which did not significantly differ from that of wild-type controls, the potentiation decayed more rapidly in knockout animals than in wild-type animals (Fig. 6A). Significant differences in the fEPSPs were observed from 2 h onwards in potentiated slices. Recorded POP spike amplitudes followed a similar time course, with significant differences between wild-type and mutant animals after 150 min posttetanization ($P < 0.05$; $n = 10$) (data not shown). To further investigate potential synaptic deficits in neurocan knockout mice, hippocampal slices were perfused for 30 min with the GABA receptor antagonist PTX. Application of PTX produced a nearly threefold potentiation of CA1 neurons. Also in this paradigm, potentiation appeared to decline more rapidly in knockout mice than in wild-type mice. However, the difference was not significant (Fig. 6B).

Taken together, these data suggest that while development, anatomy, and general performance of neurocan-deficient mice are normal, mild deficits may occur in synaptic plasticity.

DISCUSSION

Neurocan is expressed in mouse brain during embryogenesis starting at E10 and peaking around birth. Postnatally, neurocan expression is slowly reduced, and increasing proteolytic

FIG. 4. LacZ staining for the NC*LacZ*-targeted strain and immunohistochemistry for the NC*Cre*-targeted strain in the hippocampus using antibodies against neurocan, brevican, and tenascin-C. The LacZ-positive signal is observed in the granular layer of dentate gyrus and CA1 to CA3 region of the hippocampal formation (B). (A) LacZ staining in wild-type hippocampus served as a control. (C) Neurocan staining in wild-type hippocampus is present in the molecular layer of the dentate gyrus. (D) Neurocan staining in homozygous mutant mouse. There is no positive signal visible. The positive signals for brevican (E) and tenascin-C (G) are visualized in the molecular layer of the dentate gyrus in wild-type hippocampus. The expression patterns of brevican (F) and tenascin-C (H) in homozygous mutant (−/−) mice are similar to those in the wild type (+/+). (I and J) *W. floribunda* lectin (WFA) staining of perineuronal nets in the cortex of wild-type (I) and homozygous mutant (J) mice. (K and L) Electron micrographs of the synaptic neuropil of the hippocampal CA1 region of wild-type (K) and neurocan-deficient (L) mice. Asterisks represent presynaptic boutons; arrows point to postsynaptic densities of excitatory synapses. Scale bars A and B, 225 μm; C, D, E, F, G, and H, 100 μm; I and J, 100 μm; K and L, 0.5 μm.

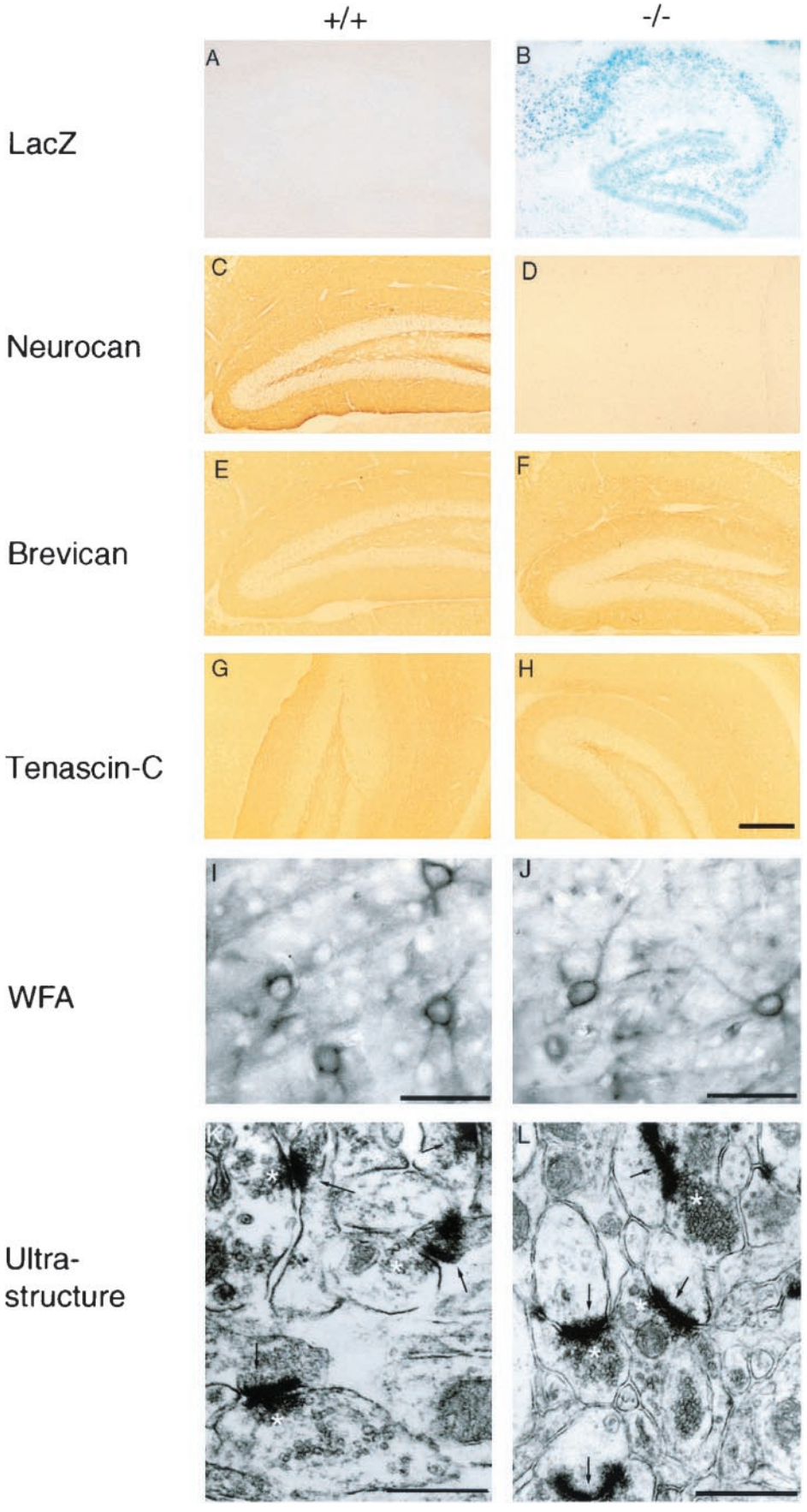
+/+
-/-
LacZ
Neurocan
Brevican
Tenascin-C
WFA
Ultra-
structure
A
B
C
D
E
F
G
H
I
J
K
L

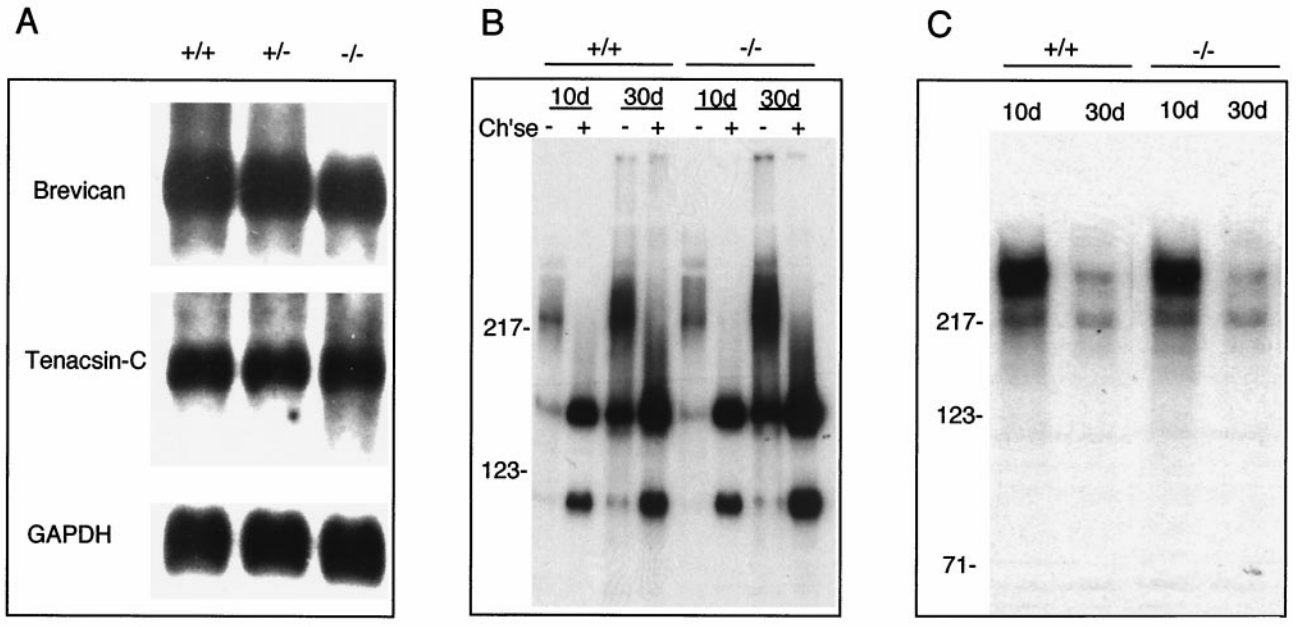

FIG. 5. Northern blot and Western blot analysis of brevican and tenascin-C genes and proteins from NC*Cre*-targeted animals. (A) Northern blot hybridizations of brevican and tenascin-C genes derived from wild-type (+/+), heterozygous (+/−), and homozygous (−/−) mice. GAPDH is a loading control. (B and C) Western blot of D10 and D30 soluble brain extract (B) and total homogenate (C) of wild-type (+/+) and mutant mice (−/−) detected by antisera against brevican (B) and tenascin-C (C), respectively. (B) Samples were treated with (+) and without (−) chondroitinase ABC (ch'se).

processing of the neurocan protein can be observed. This, however, is less obvious in mouse than in rat (34, 39). Neurocan message and protein were found in many parts of the brain, but not ubiquitously (6, 22). Neurocan can bind to N-CAM, Ng-CAM, and axonin and interfere with the cell adhesive function of Ng-CAM (10, 27, 42). In vitro experiments showed a direct repulsive effect of neurocan on neurons and an inhibition of neurite outgrowth (8), suggesting that developmentally regulated neurocan expression in certain regions of the brain will have a significant impact on axon guidance and fasciculation. In addition, neurocan is supposed to be part of a proteoglycan-hyaluronic acid network in the brain by binding to tenascin-C and, facilitated by the link protein, hyaluronic acid (11, 38). Altogether these data suggested that neurocan plays an important role during brain development, especially in axonal growth, and perhaps also in maintaining brain structure as an integral part of the brain extracellular matrix.

However, the results from neurocan-null mice indicate that the neurocan function in brain is more subtle. Neurocan-null mice were viable and fertile, had a normal life span, and showed no obvious morphological aberrations. Furthermore, no striking behavioral defects were observed when handling the mice. These data clearly show that neurocan is not essential for most if at all any axon guidance processes, since otherwise severe defects in brain morphology and basic central nervous system functions should be apparent. Neurocan is also not essential for the formation and maintenance of brain extracellular matrix, because structural integrity of the brain is not perturbed by the loss of neurocan.

An explanation for the normal phenotype of neurocan-deficient mice could be the redundant function of other proteins in the brain. Most likely candidates for such molecules are the other members of the lectican family, aggrecan, versican, and brevican (50), and also phosphacan, a brain chondroitin sulfate proteoglycan not phylogenetically related to neurocan (17, 18). All three lecticans are expressed in brain, bind to hyaluronan, and have a C-type lectin-like domain (26, 50). None of them, however, has exactly the same expression pattern or the same interacting molecules as neurocan (1). Mouse cartilage deficiency (*mcd*) mice carry a mutation in the aggrecan gene, resulting in a severely truncated molecule (46). Homozygous *mcd* mice die at birth and have a cleft palate and chondrodysplasia (47, 48). No brain phenotype was reported. Heart defect mice (*hdf*) have an insertional mutation of the versican gene. Homozygous *hdf* mice die at E10.5 and exhibit specific defects along the anterior-posterior cardiac axis (29). No brevican-null mice have been reported yet, and it is not yet clear whether there are further members of the lectican family. Candidate proteins are pgT1 (13) and the molecule(s) recognized by the monoclonal antibodies Cat-301, Cat-315, and Cat-316 (15). Various overlaps with respect to interacting molecules and expression have been shown for neurocan and phosphacan (9, 11, 24). Phosphacan is an alternative splicing product of the receptor-type protein tyrosine phosphatase that comprises the whole extracellular domain (21). While the domain structure of the proteoglycan phosphacan is rather different from that of neurocan, it is expressed during brain development and binds with high affinity to N-CAM, Ng-CAM, axonin, and tenascin-C (17). As with neurocan, phosphacan was shown to be an inhibitor of neuronal and glial adhesion and of neurite outgrowth (25).

A second explanation for the phenotype of the neurocan-null mice could be that the loss of neurocan is compensated for by increased expression of related or interacting proteins.

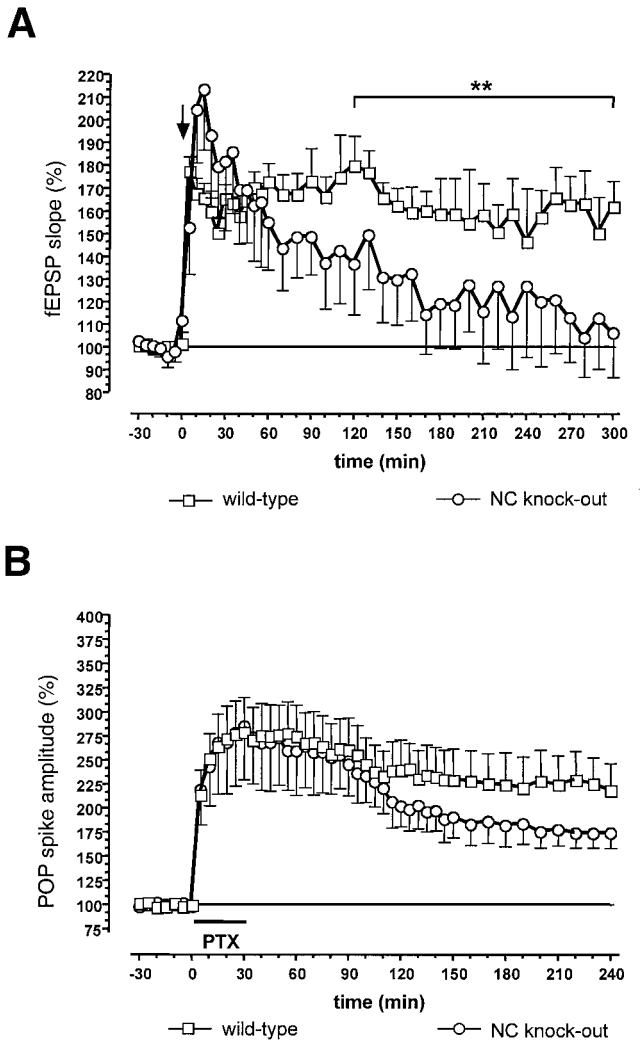

FIG. 6. Electrophysiological characterization of neurocan-deficient mice. (A) LTP. Time course of the fEPSP slope potentiation after threefold tetanization of the hippocampal Schaffer collaterals from neurocan-deficient mice (circles) compared to wild-type mice (squares). Asterisks indicate significant deviation between the wild-type group and the knockout group ($P < 0.02$ [Mann-Whitney U test]; $n = 10$). Error bars show standard errors of the means. The arrow indicates tetanization. (B) PTX induces a potentiation of the POP spike amplitude in neurcan-deficient mice (circles) and wild-type mice (squares). After stable baseline recordings, 50 μM PTX was applied to the bath containing ACSF. Immediately thereafter, potentiation of the POP spike was found; observed differences are not significant ($n = 6$). During drug application multiple POP spikes were recorded as an indication of PTX-induced afterdischarges, which to a lesser extent continued until the experiments ended.

However, testing mRNA expression of brevican and of the neurocan binding molecule tenascin-C, we could not detect any change in expression in the absence of neurocan. In addition, immunostaining of brevican and tenascin-C in brain sections showed a similar distribution in neurocan-null and control mice. Also quite similar was the relative amount of tenascin-C and brevican protein in the brain of neurocan-null mice; at least the difference was not enough to conclude that the loss of neurocan was compensated for by one of these molecules alone. However, it is still possible that other molecules of the lectican family compensate for the loss of neurocan more significantly.

Hyaluronan-proteoglycan networks with neurocan binding to hyaluronan and to tenascin-C have been proposed to describe the extracellular matrix of the brain (37). In such networks the loss of neurocan has perhaps only minor consequences, because multiple interactions between different partners exist, so that no single proteoglycan is essential for the formation and maintenance of the network. Nevertheless, absence of neurocan would have been expected to lead to a modification of the properties of the brain matrix.

Could there be any essential biological role for neurocan in the brain? Neurocan-null mice could have deficits in nonvital (at least for caged mice) brain functions like learning and memory and quantitative aberrations in behavioral model systems. This hypothesis is supported by the electrophysiological data presented here. Although basic synaptic transmission and initial potentiation appear to be normal, maintenance of the enhanced transmission is disturbed, which could be correlated with long-term memory deviations. The fact that ablation of the neurocan gene results only in a minor electrophysiological phenotype could be due to the pleiotropic character of hippocampal LTP that is affected by a number of variables, which offers the possibility of compensation. Therefore, LTP studies with double knockouts of different family members could help to unravel the putative role of the lectican family in synaptic plasticity.

After producing a lesion of the entorhinal cortex, reexpression of neurocan has been observed in zones showing remodeling of the tissue (5, 12). Thus, although neurocan is dispensable for the development of the brain, it could be of importance in restorational phases after acute brain diseases or other situations where remodeling of the tissue would be involved.

In conclusion, neurocan is not of crucial importance for brain formation and maintenance in general. However, it might play a more subtle role in brain function. Possible redundancy among lecticans or phosphacan should be tested in the future by generating double knockouts, e.g., of neurocan and brevican. Since aggrecan and versican gene ablations seem to result in early lethality, these genes have to be disrupted in a tissue-specific manner before crossing with neurocan-null mice.

ACKNOWLEDGMENTS

We thank Rupert Timpl for the generation of antibodies, Monika Marunde and Karin Schulzeck for expert technical assistance, and Michael Dictor for careful reading of the manuscript.

Xiao-Hong Zhou is a Bluecher Fellow. This work was supported by the Max-Planck Society, the DFG, and the Swedish National Research Foundation.

REFERENCES

1. **Aspberg, A., S. Adam, G. Kostka, R. Timpl, and D. Heinegard.** 1999. Fibulin-1 is a ligand for the C-type lectin domains of aggrecan and versican. J. Biol. Chem. **274:**20444–20449.
2. **Auffray, C., and F. Rougeon.** 1980. Purification of mouse immunoglobulin heavy-chain messenger RNAs from total myeloma tumor RNA. Eur. J. Biochem. **107:**303–314.
3. **Brückner, G., J. Grosche, S. Schmidt, W. Hartig, R. U. Margolis, B. Delpech, C. I. Seidenbecher, R. Czaniera, and M. Schachner.** 2000. Postnatal development of perineuronal nets in wild-type mice and in a mutant deficient in tenascin-R. J. Comp. Neurol. **428:**616–629.

4. **Celio, M. R., R. Spreafico, S. De Biasi, and L. Vitellaro-Zuccarello.** 1998. Perineuronal nets: past and present. Trends Neurosci. **21:**510–515.
5. **Deller, T., C. A. Haas, and M. Frotscher.** 2000. Reorganization of the rat fascia dentata after a unilateral entorhinal cortex lesion. Role of the extracellular matrix. Ann. N. Y. Acad. Sci. **911:**207–220.
6. **Engel, M., P. Maurel, R. U. Margolis, and R. K. Margolis.** 1996. Chondroitin sulfate proteoglycans in the developing central nervous system. I. Cellular sites of synthesis of neurocan and phosphacan. J. Comp. Neurol. **366:**34–43.
7. **Fässler, R., M. Pfaff, J. Murphy, A. A. Noegel, S. Johansson, R. Timpl, and R. Albrecht.** 1995. Lack of β 1 integrin gene in embryonic stem cells affects morphology, adhesion, and migration but not integration into the inner cell mass of blastocysts. J. Cell Biol. **128:**979–988.
8. **Friedlander, D. R., P. Milev, L. Karthikeyan, R. K. Margolis, R. U. Margolis, and M. Grumet.** 1994. The neuronal chondroitin sulfate proteoglycan neurocan binds to the neural cell adhesion molecules Ng-CAM/L1/NILE and N-CAM, and inhibits neuronal adhesion and neurite outgrowth. J. Cell Biol. **125:**669–680.
9. **Grumet, M., A. Flaccus, and R. U. Margolis.** 1993. Functional characterization of chondroitin sulfate proteoglycans of brain: interactions with neurons and neural cell adhesion molecules. J. Cell Biol. **120:**815–824.
10. **Grumet, M., D. R. Friedlander, and T. Sakurai.** 1996. Functions of brain chondroitin sulfate proteoglycans during developments: interactions with adhesion molecules. Perspect. Dev. Neurobiol. **3:**319–330.
11. **Grumet, M., P. Milev, T. Sakurai, L. Karthikeyan, M. Bourdon, R. K. Margolis, and R. U. Margolis.** 1994. Interactions with tenascin and differential effects on cell adhesion of neurocan and phosphacan, two major chondroitin sulfate proteoglycans of nervous tissue. J. Biol. Chem. **269:** 12142–12146.
12. **Haas, C. A., U. Rauch, N. Thon, T. Merten, and T. Deller.** 1999. Entorhinal cortex lesion in adult rats induces the expression of the neuronal chondroitin sulfate proteoglycan neurocan in reactive astrocytes. J. Neurosci. **19:**9953–9963.
13. **Iwata, M., T. N. Wight, and S. S. Carlson.** 1993. A brain extracellular matrix proteoglycan forms aggregates with hyaluronan. J. Biol. Chem. **268:**15061–15069.
14. **Katoh-Semba, R., M. Matsuda, K. Kato, and A. Oohira.** 1995. Chondroitin sulphate proteoglycans in the rat brain: candidates for axon barriers of sensory neurons and the possible modification by laminin of their actions. Eur. J. Neurosci. **7:**613–621.
15. **Lander, C., P. Kind, M. Maleski, and S. Hockfield.** 1997. A family of activity-dependent neuronal cell-surface chondroitin sulfate proteoglycans in cat visual cortex. J. Neurosci. **17:**1928–1939.
16. **Li, H., T. C. Leung, S. Hoffman, J. Balsamo, and J. Lilien.** 2000. Coordinate regulation of cadherin and integrin function by the chondroitin sulfate proteoglycan neurocan. J. Cell Biol. **149:**1275–1288.
17. **Margolis, R. K., U. Rauch, P. Maurel, and R. U. Margolis.** 1996. Neurocan and phosphacan: two major nervous tissue-specific chondroitin sulfate proteoglycans. Perspect. Dev. Neurobiol. **3:**273–290.
18. **Margolis, R. U., and R. K. Margolis.** 1997. Chondroitin sulfate proteoglycans as mediators of axon growth and pathfinding. Cell Tissue Res. **290:**343–348.
19. **Matsui, F., E. Watanabe, and A. Oohira.** 1994. Immunological identification of two proteoglycan fragments derived from neurocan, a brain-specific chondroitin sulfate proteoglycan. Neurochem. Int. **25:**425–431.
20. **Matthies, H., A. Becker, H. Schroeder, J. Kraus, V. Hollt, and M. Krug.** 1997. Dopamine D1-deficient mutant mice do not express the late phase of hippocampal long-term potentiation. Neuroreport **8:**3533–3535.
21. **Maurel, P., U. Rauch, M. Flad, R. K. Margolis, and R. U. Margolis.** 1994. Phosphacan, a chondroitin sulfate proteoglycan of brain that interacts with neurons and neural cell-adhesion molecules, is an extracellular variant of a receptor-type protein tyrosine phosphatase. Proc. Natl. Acad. Sci. USA **91:** 2512–2516.
22. **Meyer-Puttlitz, B., E. Junker, R. U. Margolis, and R. K. Margolis.** 1996. Chondroitin sulfate proteoglycans in the developing central nervous system. II. Immunocytochemical localization of neurocan and phosphacan. J. Comp. Neurol. **366:**44–54.
23. **Meyer-Puttlitz, B., P. Milev, E. Junker, I. Zimmer, R. U. Margolis, and R. K. Margolis.** 1995. Chondroitin sulfate and chondroitin/keratan sulfate proteoglycans of nervous tissue: developmental changes of neurocan and phosphacan. J. Neurochem. **65:**2327–2337.
24. **Milev, P., A. Chiba, M. Haring, H. Rauvala, M. Schachner, B. Ranscht, R. K. Margolis, and R. U. Margolis.** 1998. High affinity binding and overlapping localization of neurocan and phosphacan/protein-tyrosine phosphatase-zeta/beta with tenascin-R, amphoterin, and the heparin-binding growth-associated molecule. J. Biol. Chem. **273:**6998–7005.
25. **Milev, P., D. R. Friedlander, T. Sakurai, L. Karthikeyan, M. Flad, R. K. Margolis, M. Grumet, and R. U. Margolis.** 1994. Interactions of the chondroitin sulfate proteoglycan phosphacan, the extracellular domain of a receptor-type protein tyrosine phosphatase, with neurons, glia, and neural cell adhesion molecules. J. Cell Biol. **127:**1703–1715.
26. **Milev, P., P. Maurel, A. Chiba, M. Mevissen, S. Popp, Y. Yamaguchi, R. K. Margolis, and R. U. Margolis.** 1998. Differential regulation of expression of hyaluronan-binding proteoglycans in developing brain: aggrecan, versican, neurocan, and brevican. Biochem. Biophys. Res. Commun. **247:**207–212.
27. **Milev, P., P. Maurel, M. Haring, R. K. Margolis, and R. U. Margolis.** 1996. TAG-1/axonin-1 is a high-affinity ligand of neurocan, phosphacan/protein-tyrosine phosphatase-zeta/beta, and N-CAM. J. Biol. Chem. **271:**15716–15723.
28. **Miura, R., A. Aspberg, I. M. Ethell, K. Hagihara, R. L. Schnaar, E. Ruoslahti, and Y. Yamaguchi.** 1999. The proteoglycan lectin domain binds sulfated cell surface glycolipids and promotes cell adhesion. J. Biol. Chem. **274:** 11431–11438.
29. **Mjaatvedt, C. H., H. Yamamura, A. A. Capehart, D. Turner, and R. R. Markwald.** 1998. The Cspg2 gene, disrupted in the hdf mutant, is required for right cardiac chamber and endocardial cushion formation. Dev. Biol. **202:** 56–66.
30. **Mörgelin, M., D. Heinegård, J. Engel, and M. Paulsson.** 1994. The cartilage proteoglycan aggregate: assembly through combined protein-carbohydrate and protein-protein interactions. Biophys. Chem. **50:**113–128.
31. **Moser, M., T. Stempfl, Y. Li, P. Glynn, R. Buttner, and D. Kretzschmar.** 2000. Cloning and expression of the murine sws/NTE gene. Mech. Dev. **90:** 279–282.
32. **Novak, U., and A. H. Kaye.** 2000. Extracellular matrix and the brain: components and function. J. Clin. Neurosci. **7:**280–290.
33. **Oleszewski, M., S. Beer, S. Katich, C. Geiger, Y. Zeller, U. Rauch, and P. Altevogt.** 1999. Integrin and neurocan binding to L1 involves distinct Ig domains. J. Biol. Chem. **274:**24602–24610.
34. **Oohira, A., F. Matsui, E. Watanabe, Y. Kushima, and N. Maeda.** 1994. Developmentally regulated expression of a brain specific species of chondroitin sulfate proteoglycan, neurocan, identified with a monoclonal antibody IG2 in the rat cerebrum. Neuroscience **60:**145–157.
35. **Pearlman, A. L., and A. M. Sheppard.** 1996. Extracellular matrix in early cortical development. Prog. Brain Res. **108:**117–134.
36. **Potocnik, A. J., C. Brakebusch, and R. Fassler.** 2000. Fetal and adult hematopoietic stem cells require β1 integrin function for colonizing fetal liver, spleen, and bone marrow. Immunity **12:**653–663.
37. **Rauch, U.** 1997. Modeling an extracellular environment for axonal pathfinding and fasciculation in the central nervous system. Cell Tissue Res. **290:** 349–356.
38. **Rauch, U., A. Clement, C. Retzler, L. Frohlich, R. Fassler, W. Gohring, and A. Faissner.** 1997. Mapping of a defined neurocan binding site to distinct domains of tenascin-C. J. Biol. Chem. **272:**26905–26912.
39. **Rauch, U., P. Gao, A. Janetzko, A. Flaccus, L. Hilgenberg, H. Tekotte, R. K. Margolis, and R. U. Margolis.** 1991. Isolation and characterization of developmentally regulated chondroitin sulfate and chondroitin/keratan sulfate proteoglycans of brain identified with monoclonal antibodies. J. Biol. Chem. **266:**14785–14801.
40. **Rauch, U., B. Grimpe, G. Kulbe, I. Arnold-Ammer, D. R. Beier, and R. Fässler.** 1995. Structure and chromosomal localization of the mouse neurocan gene. Genomics **28:**405–410.
41. **Rauch, U., L. Karthikeyan, P. Maurel, R. U. Margolis, and R. K. Margolis.** 1992. Cloning and primary structure of neurocan, a developmentally regulated, aggregating chondroitin sulfate proteoglycan of brain. J. Biol. Chem. **267:**19536–19547.
42. **Retzler, C., W. Gohring, and U. Rauch.** 1996. Analysis of neurocan structures interacting with the neural cell adhesion molecule N-CAM. J. Biol. Chem. **271:**27304–27310.
43. **Retzler, C., H. Wiedemann, G. Kulbe, and U. Rauch.** 1996. Structural and electron microscopic analysis of neurocan and recombinant neurocan fragments. J. Biol. Chem. **271:**17107–17113.
44. **Tisay, K. T., and B. Key.** 1999. The extracellular matrix modulates olfactory neurite outgrowth on ensheathing cells. J. Neurosci. **19:**9890–9899.
45. **Watanabe, E., S. Aono, F. Matsui, Y. Yamada, I. Naruse, and A. Oohira.** 1995. Distribution of a brain-specific proteoglycan, neurocan, and the corresponding mRNA during the formation of barrels in the rat somatosensory cortex. Eur. J. Neurosci. **7:**547–554.
46. **Watanabe, H., K. Kimata, S. Line, D. Strong, L. Y. Gao, C. A. Kozak, and Y. Yamada.** 1994. Mouse cartilage matrix deficiency (cmd) caused by a 7 bp deletion in the aggrecan gene. Nat. Genet. **7:**154–157.
47. **Watanabe, H., K. Nakata, K. Kimata, I. Nakanishi, and Y. Yamada.** 1997. Dwarfism and age-associated spinal degeneration of heterozygote cmd mice defective in aggrecan. Proc. Natl. Acad. Sci. USA **94:**6943–6947.
48. **Watanabe, H., Y. Yamada, and K. Kimata.** 1998. Roles of aggrecan, a large chondroitin sulfate proteoglycan, in cartilage structure and function. J. Biochem. (Tokyo) **124:**687–693.
49. **Yamada, H., K. Watanabe, M. Shimonaka, and Y. Yamaguchi.** 1994. Molecular cloning of brevican, a novel brain proteoglycan of the aggrecan/versican family. J. Biol. Chem. **269:**10119–10126.
50. **Yamaguchi, Y.** 2000. Lecticans: organizers of the brain extracellular matrix. Cell Mol. Life Sci. **57:**276–289.